THE MICROSTRUCTURES OF SULFIDE GRAINS FROM THE VICÊNCIA LL3.2, HAMLET LL4, AND APPLEY BRIDGE LL6 CHONDRITES. T. J. Zega[1] and D. L. Schrader[2], [1]Lunar and Planetary Laboratory, 1629 E. University Blvd., Tucson AZ 85721 (tzega@lpl.arizona.edu). [2]Center for Meteorite Studies, School of Earth and Space Exploration, Arizona State University, Tempe, AZ 85287, USA (devin.schrader@asu.edu).

Introduction: Sulfides occur in a variety of planetary materials. They have been identified in meteorites, interplanetary dust particles, cometary samples, and asteroidal materials [e.g., 1–4]. Their compositions, textures, and crystal structures can be sensitive to the conditions under which they formed or last equilibrated. Thus, sulfides have been used to constrain a variety of processes including aqueous alteration, thermal metamorphism, impact shock, and crystallization as well as the oxygen and sulfur fugacities they record [e.g., 5–7].

Here we report on several sulfide assemblages from the Vicência (LL3.2), Hamlet (LL4), and Appley Bridge (LL6) chondrites. This work is part of a broader effort to determine the microstructures and origins of sulfide grains in primitive meteorites. The goal is to use this information as context for inferring the origins of sulfides in other planetary materials [7,8] including those already returned from asteroid Itokawa or those we anticipate will be returned by Hayabusa2 and OSIRIS-REx [9,10].

Samples and Methods: Petrographic thin sections of the Vicência ASU 1996 (LL3.2), Hamlet ASU 1194_C_2 (LL4), and Appley Bridge USNM614-3 (LL6) chondrites were examined using optical microscopy and electron microprobe analysis (EMPA) to locate sulfide grains as well as determine petrography, shock stage, and major element composition [7]. One assemblage in each of the three samples was selected for more detailed examination based on representative sulfide morphology, compositions, and containing both pyrrhotite and pentlandite. Electron-transparent sections were created using the Thermo Fisher (formerly FEI) Helios G^3 focused-ion-beam scanning-electron microscope (FIB-SEM) at the Lunar and Planetary Laboratory (LPL) with methods previously described [11]. Each FIB section was examined for its structure and composition using the 200 keV Hitachi HF5000 scanning transmission electron microscope (S/TEM) located at LPL. The HF5000 is equipped with a cold field-emission gun, a 3rd-order spherical-aberration corrector for STEM mode, bright field (BF)- and dark-field (DF)-STEM detectors, and an Oxford Instruments X-Max N 100 TLE EDS system with dual 100 mm^2 windowless silicon-drift detectors (Ω = 2.0 sr).

Results: Numerous sulfide assemblages were identified via optical microscopy and EMPA. Many of the assemblages contain grains large enough for phase identification via EMPA and so are designated accordingly. The results of these analyzes are discussed in [7]. However, some grains are below the 3-μm excitation volume of EMPA and preclude proper compositional identification. In particular, pentlandite exsolution in pyrrhotite is commonly below the interaction volume of the EMPA. We report details on three of them here.

Vicência opaque assemblage number 2 (OA2) occurs along the periphery of a type-II chondrule and contains subhedral pyrrhotite and pentlandite. *Hamlet* OA2 occurs on the edge of a type-II chondrule and contains subhedral pentlandite within pyrrhotite. *Appley Bridge* OA1 contains pyrrhotite and pentlandite along the edge of a taenite assemblage that contains metallic Cu and a Co-rich Fe,Ni metal phase [7]. The pentlandite contains a subhedral domain with mottled contrast, as revealed by backscatter-electron (BSE) imaging (Fig. 1a), suggesting a mixture of pentlandite and pyrrhotite. Using FIB-SEM, we deposited protective capping layers of C on top of the assemblages in orientations that transect the pyrrhotite and pentlandite interfaces. Sections were extracted in situ and thinned to electron transparency for TEM analysis.

STEM imaging shows that the section of Vicência is polyphasic. High-angle annular-dark-field (HAADF) imaging reveals that it is dominated by a high-Z material and contains smaller domains of relatively lower Z-contrast. STEM-EDS mapping indicates an Fe-Ni rich grain approximately 2.5 μm × 3 μm occurs at the surface. Measurement of a selected-area electron-diffraction (SAED) pattern is consistent with and indexes to pentlandite [110]. The pentlandite is surrounded by polycrystalline pyrrhotite. SAED patterns acquired from the pyrrhotite are a best match to the 2C polytype. Silicates, from the matrix, occur on the edge of the section.

STEM-HAADF imaging of the section of *Hamlet* reveals minor Z-contrast variations. EDS mapping shows these variations to be Ni-rich and Ni-poor domains measuring several μm in width. SAED patterns acquired from several areas in the Ni-poor domain show that it is polycrystalline pyrrhotite and measurements of one of the patterns match to the 2C polytype. The Ni-rich domain is also polycrystalline but it is currently too thick for acquisition of SAED patterns. Nonetheless, the EMPA data suggest the Ni-rich material is pentlandite.

STEM-HAADF and BF imaging show that the section of Appley Bridge is polycrystalline (Fig. 1b).

STEM-EDS mapping reveals that the section contains both Ni-rich and Ni-poor domains. The Ni-poor domains occur as micron to sub-micron laths hosted within the Ni-rich material (Fig. 1c). SAED patterns acquired from one area of the Ni-rich material indexes to pentlandite [111], whereas several from the Ni-poor material show consistency with pyrrhotite 2C. An additional Ni-poor sulfide did not precisely match the 2C polytype but has reasonable fits to 3C and 6C. It is likely an Fe-deficient pyrrhotite and additional analyses after further thinning will verify the polytype.

Discussion: The FIB sections of all three meteorites contain predominantly troilite (the 2C polytype) and pentlandite, in agreement with our previous microprobe data [7]. The microstructures of the sulfide grains in each meteorite are intriguing. Those of the Vicência (LL3.2) and Hamlet (LL4) chondrites are subhedral to anhedral, whereas that of the Appley Bridge (LL6) chondrite is euhedral and lathic. Vicência is classified as shock-stage (S) 1, Hamlet as S3, and Appley Bridge as S3. In other words, the microstructures of Vicência and Hamlet appear to be somewhat similar and not particularly remarkable regardless of their different petrologic types and shock histories. This similarity is likely due to the fact that sulfides in both Vicência and Hamlet record equilibration temperatures ≤230°C [7]. However, the abundance of Ni in pentlandite is different between LL3 and LL4 chondrites. We [7] concluded that while sulfides in Hamlet (LL4) equilibrated after thermal metamorphism, Vicência (LL3.2) may still contain primary sulfides although some low-temperature re-equilibration of some sulfides on the LL chondrite parent body could not be ruled out. The similarity of the microstructures of sulfides in Vicência and Hamlet we observe here may suggest the sulfides in Vicência were altered via low-temperature (≤230°C) metamorphism on the LL parent asteroid.

In comparison, the microstructure of Appley Bridge stands out in clear contrast to Vicência and Hamlet. We hypothesize that the lathic texture observed within the section of Appley Bridge (Fig. 1c) is a result of low-temperature exsolution of the Ni-rich pentlandite from the Ni-poor sulfide (which is almost certainly pyrrhotite) during slow cooling (discussed by [7]). Sulfides in Appley Bridge equilibrated ≤230°C, perhaps between 100 and 135°C [7]. We hypothesize that annealing led to the formation of this unique mottled pyrrhotite-pentlandite texture and pentlandite laths at low temperatures, which is why we did not observe it in the other LL3, LL4, LL5, or LL6 chondrites previously studied [7,8]. The presence of pentlandite, troilite, and Fe-deficient pyrrhotite could be an indicator of this thermal history. Whether there are any orientational relationships between the two phases, information that can be provided by SAED patterns after additional thinning, could help test this hypothesis.

Acknowledgments: We thank the Smithsonian Institution and the ASU Center for Meteorite Studies for the samples used in this study. Research funded by NASA grant NNX17AE53G (DLS PI, TJZ Co-I).

References: [1] Weisberg M. K. et al. (2006) *Meteorites and the Early Solar System II*, 19–52. [2] Bradley J. P. (2014) *Treatise on Geochemistry* 287–308. [3] Zolensky M. E. et al. (2006) *Science* 314, 1735–1739. [4] Nakamura T. et al. (2011) *Science* 333, 1113–1116. [5] Harries D. and Langenhorst F. (2013) *Meteoritics & Planet. Sci.,* 48, 879–903. [6] Schrader D. L. et al. (2016) *Geochim. Cosmochim. Acta* 189, 359–376. [7] Schrader D. L. and Zega T. J. (2019) *Geochim. Cosmochim. Acta* 264, 165–179. [8] Schrader D. L. and Zega T. J. (2019) LPS L Abstract #2009. [9] Watanabe S. et al. (2017) *Space Sci. Rev.* 208, 3–16. [10] Lauretta D. et al. (2017) *Space Sci. Rev.* 212, 925–984. [11] Zega T. J. et. al (2007) *Meteoritics & Planet. Sci., 42*, 1373–1386.

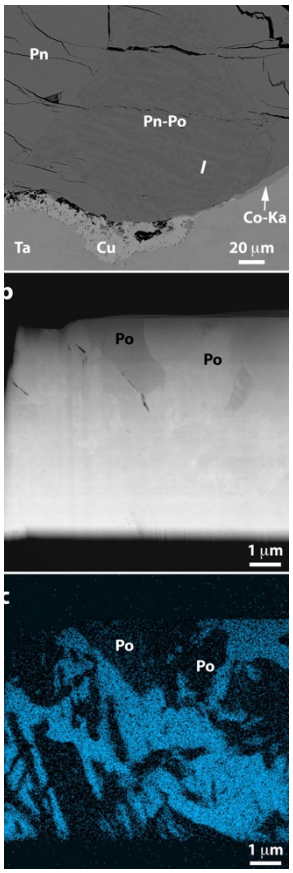

Fig. 1. EMPA and TEM data on Appley Bridge. (a) BSE image of Appley Bridge OA1. Pentlandite (Pn) and pyrrhotite (Po) occur with mottled contrast within a pentlandite bleb that has Cu metal and Co-bearing kamacite (Co-Ka) on its edge. The assemblage occurs along taenite (Ta). The FIB transect is indicated by the white line. (b) STEM-HAADF image of the FIB section. Po occurs as two polytypes and one is more Fe deficient (lower contrast) than the other. (c) STEM-EDS map of Ni Kα showing Po laths. Blue shows location of high Ni, i.e., Pn.